Cercetări Agronomice în Moldova
Vol. XLI , No. 1 (133) / 2008

CHARACTERISTICS OF MECHANICAL STRENGTH AND WATER ABSORPTION IN ALMOND AND ITS KERNEL

J. KHAZAEI*

University College of Abouraihan, University of Tehran, Iran

Received October 4, 2007

ABSTRACT *- The rupture force and energy were measured at different loading velocities, loading direction and almond size for the Mamaei variety of almond. In addition to the rupture properties, the water absorption characteristic of almond kernels was determined. Three mathematical models (Weibull, Peleg and Exponential) for describing the water absorption kinetics of almond kernels were investigated. In this study, a new model based on the time dependent viscoelastic properties of food products was proposed to describe absorption behaviour of almond kernels. The results showed that loading velocity, loading direction and almond size had significant effects on cracking force and energy. The mean values of cracking force and energy were 539 N and 443 mJ, respectively. Almond size had increasing effects on cracking force and energy. Almonds loaded from side ruptured at a lower force and energy than the ones loaded in the front orientation. The studies on water immersion showed that the rate of water uptake was maximum during the initial phase of soaking, with the moisture content of kernel increasing from 5.26% to 22.1% (dry basis) after one hour of soaking. The determined water absorption capacity (WAC, %) of almond kernels was of 1338%. Peleg, the newly developed model, and Weibull models were more accurate for describing the water absorption characteristics of almond kernels. At the very beginning times of soaking, the water absorption velocity was of 0.32 (%/min). The rate of relaxation (K_{ret} in the new developed model) was of 0.0082 (%/min).*

Key words: mechanical properties, almond, water absorption, cracking force, energy

REZUMAT – Caracteristicile forţei mecanice şi ale absorbţiei apei la migdală şi miezul acesteia. *Forţa şi energia de spargere au fost măsurate la diferite dinamici de încărcare, direcţii de încărcare şi dimensiuni ale migdalei la soiul Mamaei. În afară de forţa de spargere, s-a determinat şi absorbţia apei din miezul migdalei. Au fost testate trei modele matematice*

* E-mail: jkhazaei@ut.ac.ir

(Weibull, Peleg şi Exponențial) de descriere a cineticii de absorbție a apei din miezul de migdală. Lucrarea propune un nou model, realizat pe baza proprietăților vâscoelastice ale produselor alimentare, pentru descrierea caracterului de absorbție a miezului de migdală. Rezultatele au arătat că dinamica de încărcare, direcția de încărcare şi dimensiunile migdalei au avut efecte semnificative asupra forței şi energiei de spargere a migdalei. Valorile medii ale forței şi energiei de spargere au fost de 539 N şi, respectiv, 443 mJ. Forța şi energia de spargere sunt în concordanță cu dimensiunile migdalei. Migdalele orientate lateral au fost sparte cu o forță şi o energie mai reduse, în comparație cu cele orientate frontal. Studiile de imersie a apei au arătat că rata de absorbție a apei a fost maximă în faza inițială de înmuiere, cu un conținut de umiditate a miezului crescând de la 5,26% la 22,1%, după o oră de înmuiere. Capacitatea de absorbție a apei, determinată din miezul migdalei a fost egală cu 1338%. Noul model realizat, Peleg şi modelele Weibull au fost cele mai adecvate pentru descrierea caracteristicilor de absorbție a apei de către miezul migdalei. Rapiditatea de absorbție a apei, la începutul perioadei de înmuiere, a fost de 0.32 (%/min). Rata de relaxare (K_{ret} , la noul model realizat) a fost de 0,0082 (%/min).

Cuvinte cheie: proprietățile mecanice, migdală, absorbția apei, forța şi energia de spargere

INTRODUCTION

Almond is a dried fruit widely used, especially in the food industry. The almond kernels form an important source of energy with 6 Kcal/g, protein 15.64%, and their oil content changed from 35.27% to 40% (Abdallah et al., 1998).

After harvesting, almond is subjected to different treatments, such as cracking almonds and removing the kernels, wetting the kernels in water for about 13 hours, peeling the wet kernel, and finally, drying the peels. A significant proportion of almond production is used in the peeled form.

The mechanical properties and water absorption characteristics of almond and its kernels, like those of other fruits, grains and seeds, are essential for the design of equipment for harvesting, cracking, peeling, and processing of almond and its kernels. The development of satisfactory harvesting and processing methods are greatly influenced by the physical and mechanical properties of the product. In fact, the output of agricultural and processing machines depends on material properties.

Since they are used, the almond processing systems have been generally designed without considering these criteria, the resulting designs leading to inadequate applications. This results in a reduction in work efficiency and an increase in product loss. Therefore, determination and consideration of these criteria have an important role in designing these equipments.

Today, there are only few data in the literature describing the physical and mechanical properties of almond and its kernel. However, the mechanical and water absorption characteristics of different types of fruits, grains and seeds have

been determined by other researchers. Some mechanical properties of almond kernels, such as rupture strength and sphericity were reported by Kalyoncu (1990).

Mechanical properties of the agricultural products are most conveniently measured with the force-deformation curve. From this curve, a number of mechanical properties can be determined, such as maximum force and energy to rupture point, stiffness and deformation. Three methods have been used to obtain such force-deformation curves (Fischer et al., 1969): 1) the compression of the product by a small flat cylindrical die (plunger test), 2) the compression of fruit between two parallel flat plates (plate test) and 3) the compression of a cubic sample of product between two parallel flat plates.

Kalyoncu (1990) measured the size and rupture strength of almond nuts from 10 almond varieties, and determined the relationship between the rupture strength and the size of nuts. Oloso and Clark (1993) studied the effect of moisture content and loading direction on the rupture force, deformation and energy of roasted cashew nut under quasi-static loading. They found that all the factors examined have significantly affected the measured parameters and the pattern of cracking of the nutshell, too. Liang et al. (1984) carried out similar investigation on walnuts and found that the difference between kernel and walnut cracking deformation appeared to be a dependable indicator for predicting the effect of moisture content and compression magnitude on kernel damage. Bilanski (1966) measured the force and energy required to initiate soybean seed coat rupture. For compressing the soybean seed with the hilum in the horizontal position, the average force to initiate seed coat rupture dropped from 57.8 to 44.4 N, respectively, when seed moisture content was increased from 1% to 16%.

The effect of loading direction and nut size has been investigated by other researchers. For walnuts at 6% moisture content (wet basis), Borghei et al. (2000) reported that the cracking force and strain of walnuts were in the range of 110 to 800 N and 0.01 to 0.045 mm/mm, respectively. The study also showed that large sized walnuts required higher cracking force and experienced more deformation than small ones.

The effective design of drying and storage systems for almond kernel and its peels also needs knowledge of their absorption properties. Hence, modelling water transfer in kernels during soaking has attracted considerable attention.

Many theoretical, empirical and semi-empirical models approaches have been employed for modelling the water absorption behaviour of agricultural products during soaking. The most popular empirical and semi-empirical models (*Table 1*), which has been used to model the water absorption process of agricultural products are the Peleg model (Gowen et al., 2007; Sayar, et al., 2001; Turhan, et al., 2002), the Weibull distribution function (Garcia-Pascual et al., 2006; Machado, et al., 1999; Marabi, et al., 2003), and exponential model (Gowen et al., 2007; Kashaninejad, et al., 2007). Empirical models are often preferred to the theoretical ones, due to their ease of computability and interpretation.

Table 1 - Empirical models frequently utilized in curve fitting of water absorption data

Model	Formula	Eq.
Page	$M_t - M_o = \frac{t}{K_1 + K_2 t}$	[1]
Weibull	$Mr = \frac{M_t - M_s}{M_o - M_s} = \exp(-(\frac{t}{\beta})^{\alpha})$	[2]
Exponential	$Mr = \frac{M_t - M_s}{M_o - M_s} = \exp(-Kt)$	[3]

Water absorption behavior, like viscoelastic properties of food products, is a time- dependent behavior (*Figure 1*). Therefore, it is possible to model these two different properties of agricultural materials with the same model. According to *Figure 1*, the water absorption behavior of agricultural products may be defined as follows (Mohsenin, 1986):

$$M_t - M_o = M_{ret}(1 - e^{-t/T_{ret}}) + K_{rel}t \qquad (4)$$

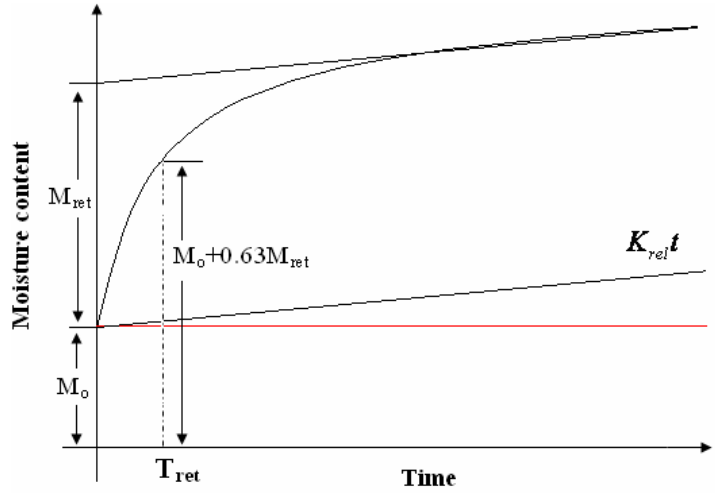

Fig. 1 - Graphical method to determine the constants of the newly developed model (Eq. [4])

Where, M_t is the moisture content t min after soaking, M_o is the initial moisture content and Krel is the rate of absorption of water in the relaxation phase (% / min). According to *Figure 1*, the time of retardation, Tret, is the time required to reach the moisture content of product to about 63% of the total absorbed moisture content, Mret (*Figure 1*). In other words, Tret shows the rate of absorption in the first phase of the process. The highest amount of Tret shows the

higher rate of water absorbance in the first phase of absorption. In addition, the Krel shows the rate of water absorption in the relaxation phase, which is calculated by determining the slope of the tangent line on the end part of sorption curve (*Figure 1*). The benefit of this model in respect with other empirical and semi- empirical models is its ability to determine all the constant parameters directly from the absorption curve. This model is also able to describe the second phase of moisture absorption, the relaxation phase.

The objectives of this study were (1) to determine the average force, deformation, and energy absorbed at rupture for almond, in both vertical and horizontal loading orientations under quasi-static compression, and (2) to determine the water absorption kinetics of almond kernels.

MATERIALS AND METHODS

Sample Preparation

Almonds of the *Mamaei* cultivar were procured from a government orchard near Shahrekord, Iran. The almonds were cleaned manually to remove foreign matter, along with broken and immature fruits. Almond were transported directly to the laboratory and stored in a refrigerator at 6.5°C.

The intact kernels were obtained by manual dehulling of these almonds. The initial moisture contents of whole almonds and kernels were 6.3% and 5.26% d.b., respectively, using the standard hot air oven method with a temperature setting of 105°C and a drying time of 24 h.

Mechanical Properties

The compression (plate) test was used to evaluate the force and energy required to rupture almond under quasi-static loading. Due to the range of the almond dimensions, it was necessary to sort almonds before performing the rupture tests. Almonds were sorted into three categories according to their thickness. The average thickness for small, medium, and large almonds was 11.5, 13.5, and 16.5 mm, respectively.

The almond samples were visually inspected prior to loading, and those with visible cracks on the hull were discarded. Thus, the results from these tests should be considered the maximum force and deformation that the hull of almond kernel can withstand prior to rupture. Quasi-static compression tests were performed with an Instron Testing Machine (Model 1186) equipped with a 5000 N compression load cell.

In this study, the effects of the following factors were studied on almond cracking force, absorbed energy and required power: loading direction (side and front), almond dimension (small, medium and large), and loading rate (5, 100, 200, 500 mm/min). Fifteen replications were used for each treatment.

Each individual almond was loaded between two parallel plates and compressed until the hull ruptured. To determine the effect of orientation of loading on rupture, almonds were positioned in either the front or in the side plane (*Figure 2*). A force-deformation curve was obtained for each almond. The absorbed energy was calculated by measuring the surface area under the force-deformation curve.

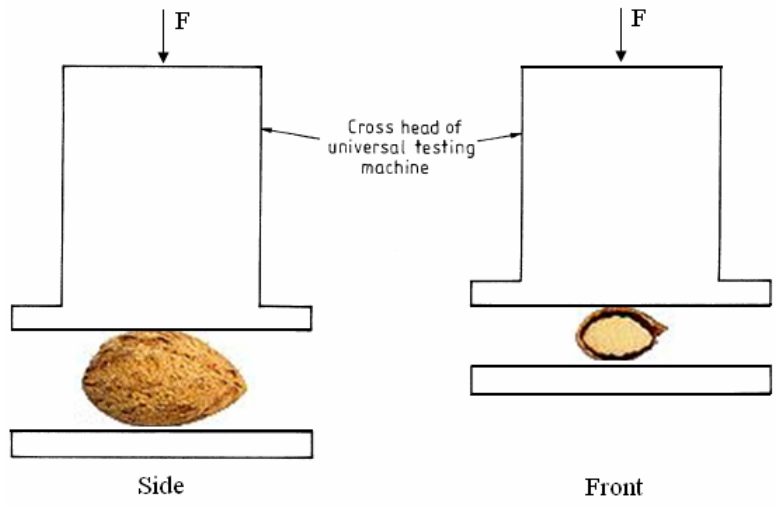

Fig. 2 - Loading direction of almond between two parallel plates

Water Absorption

The water absorption behaviour of almond kernels was determined by soaking 20 g samples, with initial moisture content of 5.26%, in cylindrical containers containing 150 ml of distilled water. The studied soaking temperature was 27°C. The temperature of water was controlled automatically by using a hardware system with an accuracy of ±0.1°C.

Sample moisture content each time after soaking was calculated based on the increase in the sample weight at corresponding times. For this purpose, at regular time intervals, ranging from 2 min at the beginning to 30 min during the last stages of the process, the kernels were rapidly removed from the test tubes and superficially dried on a large filter paper, to eliminate the surface water. The kernels were then weighed to determine the moisture uptake. The samples were subsequently returned to water via wire mesh baskets, and the process was repeated until the kernels moisture content attained a saturation moisture content, i.e., when three successive weight measurements differ from the average value in less than ±1% (Resio, et al., 2005). Tests were triplicated and the average results were used for further analysis. Using these data, the water absorption capacity (WAC) of almond kernels was determined as follows:

$$\text{Water absorption capacity } (WAC) = \frac{M_s - M_o}{M_o} \times 100 \qquad (5)$$

Where, M_s is the saturation moisture content and M_o initial moisture content. For mathematical modelling of the variation of either moisture content or moisture ratio of almond kernels during soaking, the Peleg, Weibull, Exponential models, as well as the new model introduced in Eq. [4], were tested. The parameters in each model were estimated by using the non-linear regression analysis. For this, we have used the SigmaPlot software. The performances of the models were compared, according to their coefficient of determination (R^2) and the root mean square error (RMSE, %) of the moisture content or moisture ratio (Resio et al., 2003).

RESULTS AND DISCUSSION

Mechanical Properties

The force-deformation characteristic exhibited by the whole almond under compressive loading from front is shown in *Figure 3*. The most important point of the compression curve was the first local maximum point, which was selected as the rupture force. There was a decrease in the force after rupture occurred in the specimen and this point was denoted as the rupture point.

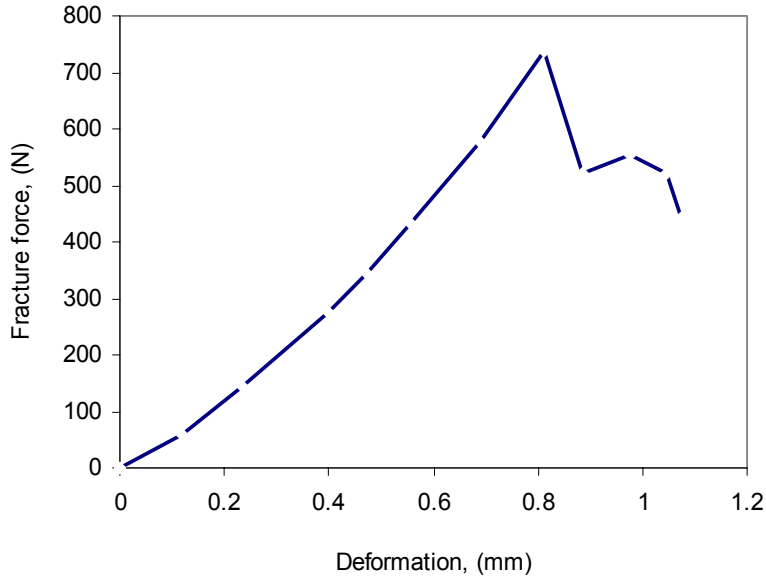

Fig. 3 - A typical force-deformation curve for almond under compressive loading from front

The results of the variance analysis showed that loading velocity, loading direction and almond size had significant effects on cracking force and energy. The mean values of parameters are presented in *Table 2*. *Table 3* shows the results of Duncan's Multiple Range Tests at 0.01 significance level for a comparison between the mean values of the cracking force and the energy required to fracture almonds at different loading rates, direction of loading and almond dimension.

Table 2 - Mean values of force and energy required for cracking almonds

Parameter	Mean	Max	Min	Std
Cracking Force, (N)	539	954	241	187
Absorbed Energy, (mJ)	443	843	260	145

Table 3 - Duncan's Multiple Range Tests to compare the mean values of cracking force and energy for almond at different loading velocity, almond size, and loading direction

Variable	Level	Cracking Force (N)	Absorbed Energy (mJ)
Loading velocity	5	673a	474a
	100	566b	418b
	200	483c	415b
	500	432c	465b
Almond size	Small	454c	330c
	Medium	562b	433b
	Large	600ab	566a
Loading direction	Side	502b	391b
	Front	575a	495a

Almond size showed a significant effect on rupture force and energy (*Figures 4-9*). *Figures 4-9* show that the cracking force increased with increasing almond dimension. The rupture force of large almonds was by 1.32 times higher than in case of small ones. The mean cracking force for large and small almonds was 600 and 454 N, respectively. Table 3 shows that the difference between the cracking force for large and medium almonds was not significant at P=0.01. The higher cracking force for large almonds may be explained by their thicker shell.

Data showed that the loading velocity had a decreasing effect on the rupture force for both loading directions (*Figures 4 and 5*). The difference between cracking force at 200 and 500 mm/min loading velocity was not significant but the effects at other loading velocities differed significantly. The rupture force decreased by 36%, while the loading velocity increased from 5 to 500 mm/min.

The direction of loading has significantly affected (P=0.01) the amount of force required to crack almonds (*Figures 4-5*). The results showed that almonds loaded from side ruptured at a lower force than the ones loaded in the front orientation. The average cracking force for loading in side and front directions were 502 and 575 N, respectively (*Table 3*). Since an externally applied force creates shear stresses in internal tissues, causing rupture of the cotyledon, and because there is a definite cellular arrangement in the cotyledon tissues, a greater or lesser force may be required to cause rupture, depending on the direction of the applied force (Peterson et al., 1995).

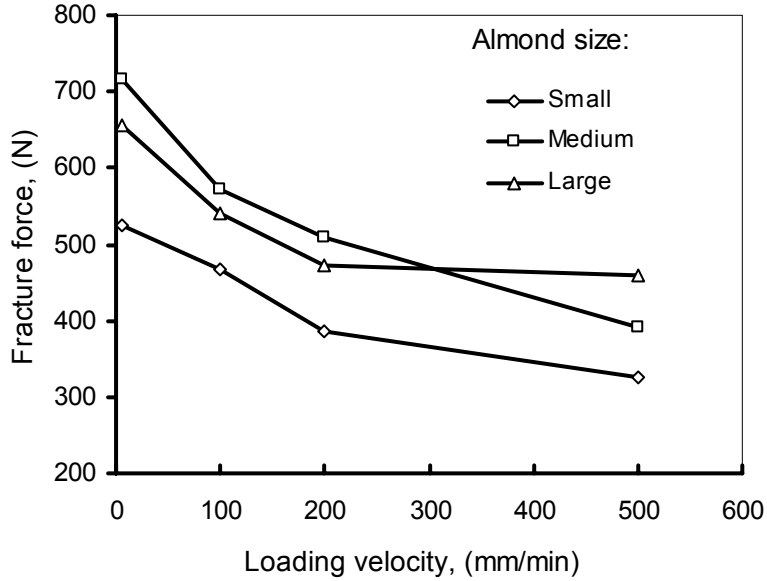

Fig. 4 - Effect of loading rate and almond dimension on the cracking force. Direction of loading from front

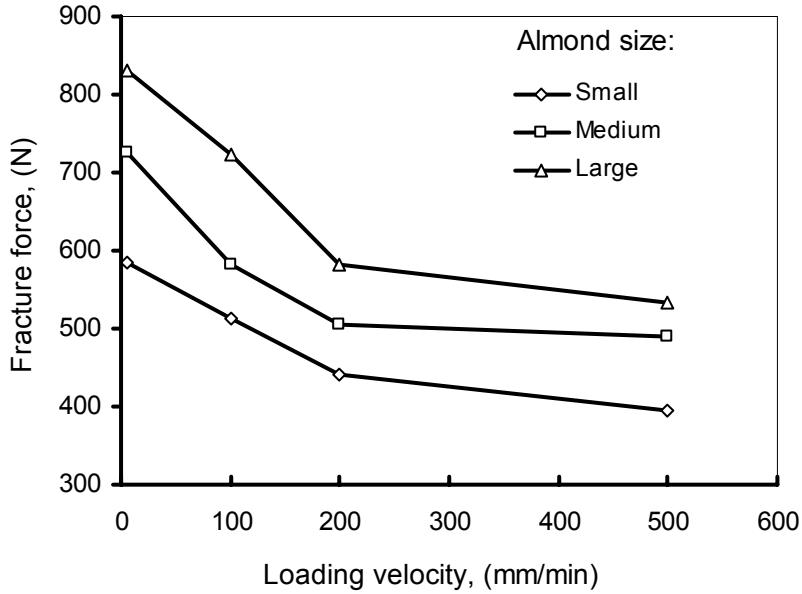

Fig. 5 - Effect of loading rate and almond dimension on cracking force Direction of loading from side

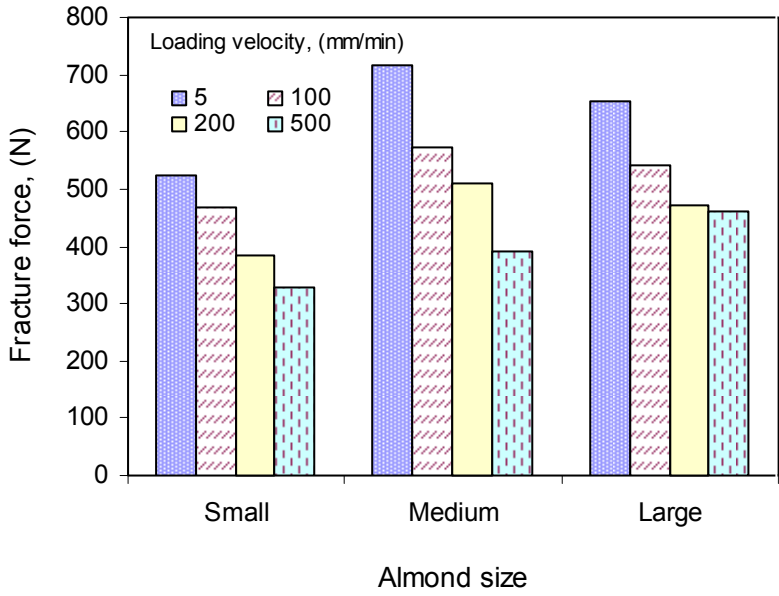

Fig. 6 - Effect of almond size on fracture force. Loading from front

Almond dimensions as well as the direction of loading have significantly affected the amount of energy required for cracking almonds. Large almonds absorbed more prior to cracking. The difference between the mean values of absorbed energy for large, medium and small size almonds were significant at P=0.01 (*Table 3*).

The direction of loading has significantly affected (P=0.01) the amount of energy required to crack almonds. It was observed that the almonds absorbed more energy before rupture when compressed in the front orientation (*Table 3*). In side loading orientations, the rupture energy of almonds increased as the almond size increased (*Figure 8*). The results showed that medium almonds loaded from front required higher energy than the large and small ones.

The average cracking energy for loading in side and front directions were 502 and 575 N, respectively. This means the chances of dehulling would be greater when there is a higher probability that the almonds receive an impact or compressive load in the side direction. *Figures 7 and 8* show that the absorbed energy for cracking almonds was reduced with the increase in the loading velocity from 5 to 200 mm/min, and then increased with higher increase in loading velocity to 500 mm/min. The difference between the mean values of cracking energy at 100, 200, and 500 mm/min loading velocities were not significant, but the differences between 5 and other levels was significant.

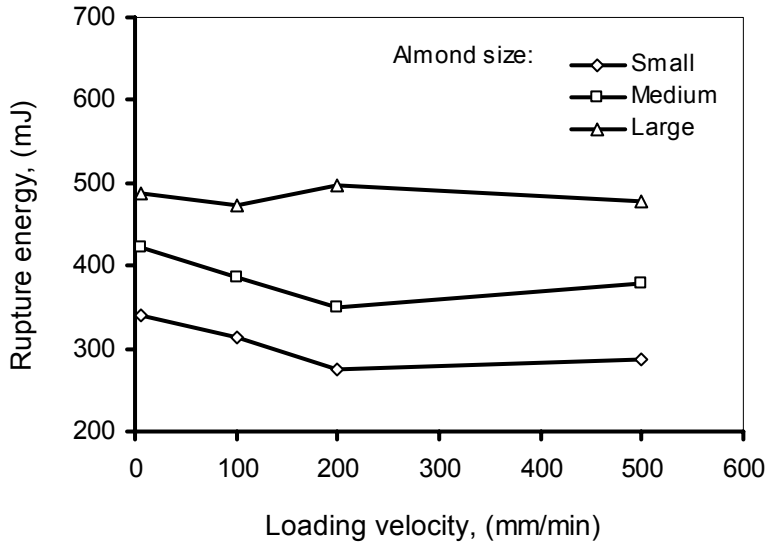

Fig. 7 - Effect of loading rate and almond dimension on the absorbed energy for cracking. Direction of loading from front

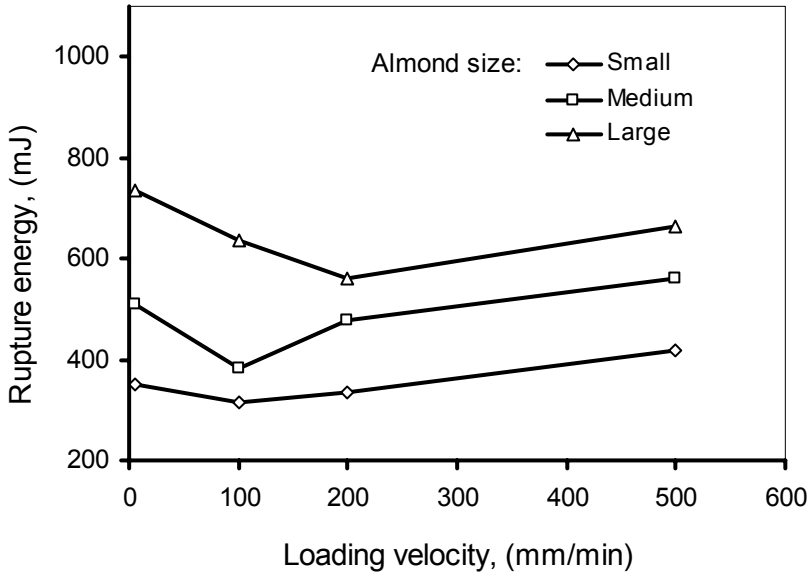

Fig. 8 - Effect of loading rate and almond dimension on absorbed energy for cracking. Direction of loading from side

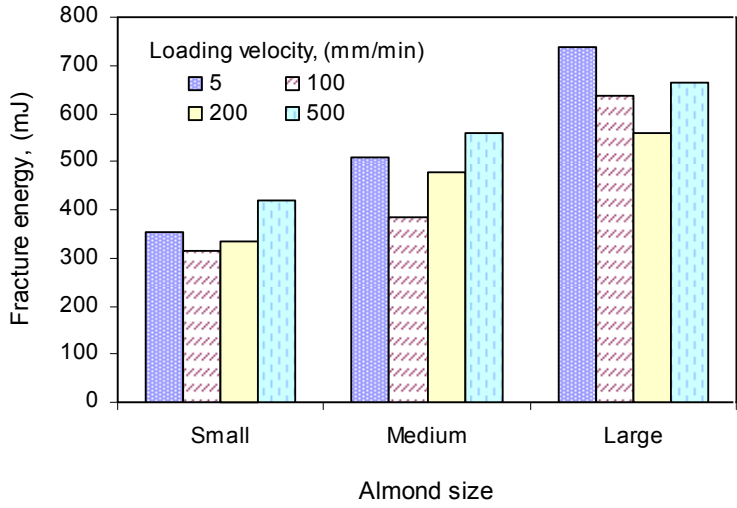

Fig. 9 - Effect of almond size on fracture force. Direction of loading from side

Water Absorption

The variation in the moisture contents of almond kernels during soaking in plain water at temperature of 27 °C is shown in *Figure 10*. The kernels exhibited an initial high rate of moisture sorption, followed by slower absorption at latter stages, the relaxation phase. Previous studies have also reported identical curves during the soaking of other grains and seeds (Abu-Ghannam and McKenna, 1997; Bello et al., 2004; Sopade et al., 1992). The water absorption capacity (%) of almond kernels, calculated by using the Eq. [5], was determined equal to 1338%.

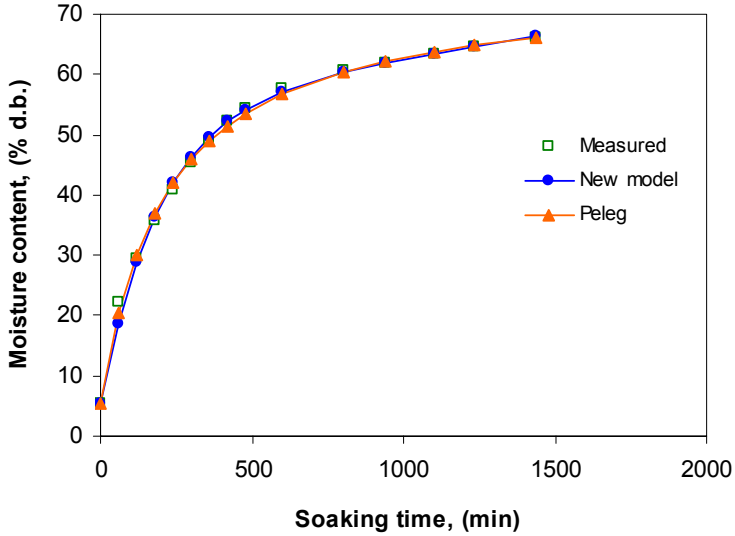

Fig. 10 - Relationship between kernel moisture content with immersion time in water

Table 4 presents the results of non-linear regression analysis of fitting the Peleg, Weibull, Exponential and the newly introduced model in Eq. [4] to the experimental data and comparison criteria, used to evaluate goodness of fit namely, R^2 and RMSE. It is evident that Peleg, the newly introduced model, and Weibull models were more accurate for describing the water absorption characteristics of almond kernels. The values of RMSE obtained from the three models were less than 5%, which are in an acceptable range. It is most likely that the water uptake process of almond kernels could be interpreted as a sequence of probabilistic events represented by the Weibull model rather than a diffusion-based process.

Table 4 - Estimation of the parameters and goodness of fit of the Peleg, Weibull, Exponential and the newly introduced model in Eq. [4], applied to moisture uptake kinetics of almond kernels

Temperature (°C)	Model					
Peleg	K1 (min / %)	K2 (1/ %)		R^2		RMSE (%)
	3.1271	0.0142		0.998		3.2
Weibull distribution function	α (min / %)	β (1/ %)		R^2		RMSE (%)
	0.6343	419.3		0.993		8.4
Exponential model	K (min / %)	R^2		RMSE (%)		
	0.0025	0.907		36.9		
Newly introduced model in Eq. [4]	Mo (% d.b)	M_{ret} (% d.b)	T_{ret} (min)	K_{rel} ($\%min^{-1}$)	R^2	RMSE (%)
	5.26	49.2	196.1	0.0082	0.996	5.3

According to the Peleg model in Eq. (1), the water absorption velocity at the very beginning times of soaking, i.e., when $t \to 0$ may be obtained by the following equation (Turhan et al., 2002):

$$R_o = \left(\frac{M_{t+dt} - M_t}{dt}\right)_{t=0} = \frac{1}{K_1} \quad (6)$$

Knowing the constant of K_1 for almond kernels, the mean value of Ro was calculated and reported in Figure 11. The figure shows that the initial slope of the sorption curve increases once with the temperature, although the water intake slows down quickly, thus reflecting a lower water effective diffusion coefficient. The reason for higher initial water absorption rate can be explained by the diffusion phenomenon. The rate of water absorption depends on the difference between the saturation moisture content and water content at a given time, which is called the driving force. As hydration proceeds, the water content increases, diminishing the driving force and consequently the sorption velocity. As the

driving force in the water movement decreases, the extraction of soluble solids in the reverse direction to the water movement offers additional resistance to water transfer as well (Abu-Ghannam and McKenna, 1997; Sayar et al., 2001). The water absorption process ceases when the kernels attain the equilibrium in water content.

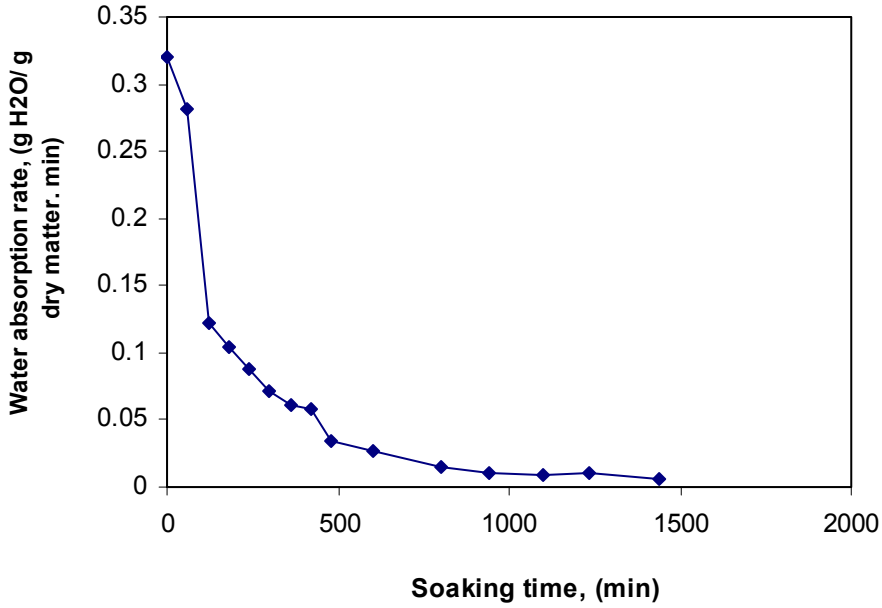

Fig. 11 - Rate of water uptake in kernel with time

REFERENCES

Abdallah A., Ahumada M.H., Gradziel T.M., 1998 - *Oil content and fatty acid composition of almond kernels from different genotypes and California production regions*. J. Am. Soc. Hort. Sci. 123:1029-1033

Abu-Ghannam N., McKenna B., 1997 - *Hydration kinetics of kidney beans* (*Phaseolus vulgaris* L.). Journal of Food Science, 62, 520–523

Bello M., Tolaba M.P., Suarez C., 2004 - *Factors affecting water uptake of rice grain during soaking*. Lebensm.-Wiss. u.-Technol, 37:811–816

Bilanski W.K., 1966 - *Damage resistance of seed grains*. Trans. ASAE. 9, 360-363

Borghei A.M., Khazaei J., Tavakoli T. - *Design, construction and testing of walnut cracker*. AgEng2000 Conference. Paper No: 00-PH-029

Garcia-Pascual P., Sanjuan N., Melis R., Mulet A., 2006 - *Morchella esculenta (morel) rehydration process modelling*. Journal of Food Engineering, 72, 346-353

Gowen A., Abu-Ghannam N., Frias J., Oliveira J., 2007 - *Influence of pre-blanching on the water absorption kinetics of soybeans*. Journal of Food Engineering, 78, 965–971

Kalyoncu I.H., 1990 - *A selection study on determining important characteristics of almond trees in Turkey*, Master thesis, University of Ondokuz Mays, Samsun, Turkey

Kashaninejad M., Maghsoudlou Y., Rafiee S., Khomeiri M., 2007 - *Study of hydration kinetics and density changes of rice (Tarom Mahali) during hydrothermal processing*. Journal of Food Engineering, 79, 1383–1390

Liang T., Chin L., Mitchell J.B., 1984 - *Modelling Moisture Influence on Macadamia nut Kernel Recovery*. Trans. ASAE. 28 :1538 – 1541

Machado M.F., Oliveira F.A.R., Cunha L.M., 1999 - *Effect of milk fat and total solids concentration on the kinetics of moisture uptake by ready-to-eat breakfast cereal*. International Journal of Food Science and Technology, 34, 47–57

Marabi A., Livings S., Jacobson M., Saguy I.S., 2003 - *Normalized Weibull distribution for modelling rehydration of food particulates.* European Food Research Technology, 217, 311–318

Mohsenin N.N., 1986 - *Physical properties of plant and animal materials*. 2nd ed. Gordon Breach Science, Publ; New York

Oloso A.O., Clarke B., 1993 - *Some Aspect of Strength Properties of Cashew Nuts*. J. Agric. Engng. Res. Vol 55: 27 – 43

Peterson J.M., Perdomo J.A., Burris J.S., 1995 - *Influence of kernel position, mechanical damage and controlled deterioration estimates on hybrid maize seed quality*. Seed Science and Technology, 23, 647±657

Resio A.N.C., Aguerre R.J., Suarez C., 2005 - *Analysis of simultaneous water absorption and water–starch reaction during soaking of amaranth grain*. Journal of Food Engineering, 68, 265–270

Resio A.N.C., Aguerre R.J., Suarez C., 2003 - *Study of some factors affecting water absorption by amaranth grain during soaking*. Journal of Food Engineering, 60, 391–396

Sayar S., Turhan M., Gunasekaran S., 2001 - *Analysis of chickpea soaking by simultaneous water transfer and water-starch reaction*. Journal of Food Engineering, 50, 91-98

Sopade P.A., Ajisegiri E.S., Badau M.H., 1992 - *The use of Peleg's equation to model water absorption in some cereal grains during soaking*. Journal of Food Engineering, 15, 269–283

Turhan M., Sayar S., Gunasekaran S., 2002 - Application of Peleg model to study water absorption in chickpea during soaking. Journal of Food Engineering, 53, 153–159